JOURNAL OF MATERIALS SCIENCE 19 (1984) 223–232

Environmental durability of aluminium adhesive joints protected with hydration inhibitors

D. A. HARDWICK, J. S. AHEARN, J. D. VENABLES
Martin Marietta Laboratories, 1450 South Rolling Road, Baltimore, Maryland 21227, USA

The effect of adsorbed inhibitor films on the durability of aluminium adherends prepared by the Forest Products Laboratory process was determined. Dilute aqueous solutions of phosphoric acid (PA) and nitrilotris (methylene) phosphonic acid (NTMP) were used. The presence of a monolayer of NTMP resulted in a four-fold increase in bond durability over that of untreated adherends. Dilute solutions of PA were ineffective in improving bond durability. Correlated wedge tests (coupled with a fracture energy analysis), surface composition determinations using X-ray photoelectron spectroscopy, and surface examination using high resolution scanning electron microscopy suggested that a compound's effectiveness in improving bond durability depends on its ability to inhibit the conversion of aluminium oxide to hydroxide and form chemical bonds with the adhesive.

1. Introduction

Adhesively bonded aluminium structures are finding increased use in numerous applications calling for a light-weight structural material. The performance of such structures is largely determined by two factors: the initial bond strength of the adherend/adhesive interface and the stability of the interface in a humid environment, i.e. the durability of the bond. Recent studies [1] have indicated that the initial bond strength of joints produced by commercial aerospace bonding processes, including the Forest Products Laboratory (FPL) process and the Boeing phosphoric acid anodization (PAA) process, is determined principally by physical interlocking of the oxide on the aluminium adherend with the adhesive. On the other hand, the long-term durability of the aluminium oxide adhesive bond appears to depend on the resistance of the original adherend oxide to conversion to a hydroxide in the presence of moisture [2].

The bond durability of adherends prepared using the PAA process is substantially better than that of adherends prepared with the FPL process. PAA oxides are considerably thicker than FPL oxides (~ 300 nm as opposed to 40 nm) but the PAA oxide also contains phosphorus in the form of a phosphate, a known inhibitor of aluminium oxide hydration [3]. In fact, recent work [4] has shown that a critical step in the hydration of PAA oxides is the dissolution of a phosphorus-rich surface layer.

It has also been demonstrated that the adsorption of phosphorus-containing compounds on to FPL aluminium oxides stabilizes the oxide by increasing the time needed to convert the original oxide into a hydroxide [5, 6]. The objective of the present work was to study the influence that adsorbed phosphorus-containing compounds have on the durability of FPL oxide/adhesive bonds. Two inhibitor species were chosen, one an organic, nitrilotris (methylene) phosphonic acid (NTMP) $N[CH_2P(O)(OH)_2]_3$, and one an inorganic, phosphoric acid. With the aid of these adsorbed inhibitors we have addressed the issue of whether surface chemistry or oxide morphology, exclusively or in combination, control bond durability.

2. Experimental techniques

2.1. Sample preparation

Test coupons and panels of 2024-T3 aluminium were degreased in a commercial alkaline cleaning

0022–2461/84 $03.00 + .12

solution and then rinsed in distilled, deionized water. A standard FPL treatment was used for all samples: 15 min immersion in an agitated, aqueous solution of sodium dichromate dihydrate ($60\,g\,l^{-1}$) and sulphuric acid (17 vol%) held at 65° C, followed by a rinse in distilled, deionized water and air drying. Some panels were then treated using the PAA process: anodization in 10 wt% phosphoric acid solution at 10 V for 20 min at 20 to 25° C.

Treatment of FPL-prepared coupons and panels with inhibitor was accomplished by immersing them for 30 min in an aqueous solution of the inhibitor held at either room temperature or 80° C, followed by rinsing in distilled, deionized water and air drying.

2.2. Wedge-test procedure

Following surface preparation, adherends (15 cm × 15 cm × 0.3 cm) were bonded together, using American Cyanamid FM 123-2 adhesive, cured at 120° C for 1 h, and cut into five 2.5 cm × 15 cm test pieces. Wedges (0.32 cm thick) were inserted between the adherends to provide a stress at the bondline. After an equilibration period of 1 h at ambient conditions, the test samples were placed in a humidity chamber held at 60° C and 98% RH and periodically removed for examination under an optical microscope. The position of the crack front at both edges of the sample was located and marked.

A wedge-test specimen is a modified double-cantilever beam (DCB) specimen. If the crack length, a, is measured from the point of load application, then it follows from simple beam theory that the load, p, can be expressed as a function of the fixed displacement, w, as [7]:

$$P = \frac{Bh^3Ew}{8a^3}, \tag{1}$$

where h is the thickness of the adherends; B, the width of the adherends; and E, Young's modulus. According to linear elastic fracture mechanics, the load is proportional to the displacement: $w = CP$, where C is the compliance of the specimen, i.e. from [1]:

$$C = \frac{8a^3}{Eh^3B}. \tag{2}$$

Using the Griffith energy criterion, G, the strain energy release rate or fracture energy is given by [7]:

$$G = \frac{P^2}{2B}\frac{dC}{da}. \tag{3}$$

Thus, from Equations 2 and 3:

$$G = \frac{3h^3Ew^2}{16a^4}. \tag{4}$$

Although this formulation neglects the compliance of the adhesive, the experiments were conducted with only the adherend surface preparation as a variable, therefore, these corrections were considered unimportant.

These equations for G assumed that bending in the adherend itself is entirely elastic. This assumption holds only when [8]:

$$G = \frac{Eh\epsilon^2}{3}, \tag{5}$$

where ϵ is the yield strain of the adherends. For 2024-T3 aluminium, which has a yield stress of 345 MPa, G must exceed $1.8\,kJ\,m^{-2}$ for plastic deformation to occur. This is in agreement with the observation that when the wedge test assemblies were broken open at the conclusion of the test the adherends were not permanently deformed.

2.3. Surface analysis – X-ray photoelectron spectroscopy (XPS)

The XPS measurements were performed with a Physical Electronics (Model 548) spectrometer consisting of a double-pass cylindrical mirror analyser with pre-retarding grids and a magnesium X-ray source. The reported surface analyses and the surface coverage data were determined from peak height measurements using sensitivity factors derived from standards [3].

2.4. Scanning electron microscopy (SEM)

Surfaces were examined in a JEOL-120CX scanning-transmission electron microscope (STEM) operated in the high resolution (2 to 3 nm) SEM mode. To suppress charging of the surface by the electron beam, an extremely thin Pt coating was deposited on the surfaces of the specimens by secondary ion deposition.

3. Results

3.1. Inhibition surface coverage

A typical XPS spectrum from an FPL surface treated in NTMP is shown in Fig. 1. Based on binding energy measurements, we determined that aluminium and most of the oxygen are derived from aluminium oxide and most of the carbon, from a surface layer of hydrocarbon contami-

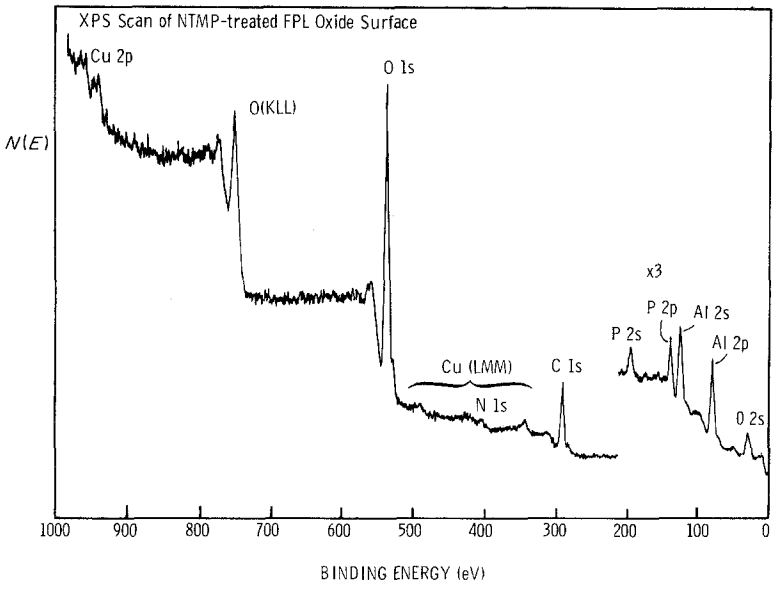

Figure 1 XPS spectra of NTMP-treated FPL oxide surface.

nation. Copper results from copper in the near-surface metal region behind the oxide surface and from copper-rich inclusions near the surface. The phosphorus, nitrogen, and some oxygen and carbon result from adsorbed NTMP molecules.

The amount of inhibitor adsorbed on a treated surface was determined by measuring the peak heights of the 2p electrons from phosphorus and aluminium and calculating the P/Al ratio. As shown in Fig. 2 for NTMP, the surface coverage saturates as the solution concentration increases above 10 ppm. The saturation surface coverage values, for room temperature treatment using NTMP and PA, and 80° C treatment for NTMP, are given in Table I. The value of 0.1 obtained for the saturation surface coverage of PA on FPL oxides is the same as the P/Al ratio obtained on PAA oxides [5].

3.2. Wedge tests

A typical plot of wedge-test data for FPL adherends treated in room temperature NTMP solutions is shown in Fig. 3. The NTMP significantly improved the durability of the FPL-etched adherends over that exhibited by untreated adherends. Indeed, the performance of the FPL adherend treated in 10 ppm NTMP approached, in this particular test, that of the PAA adherends.

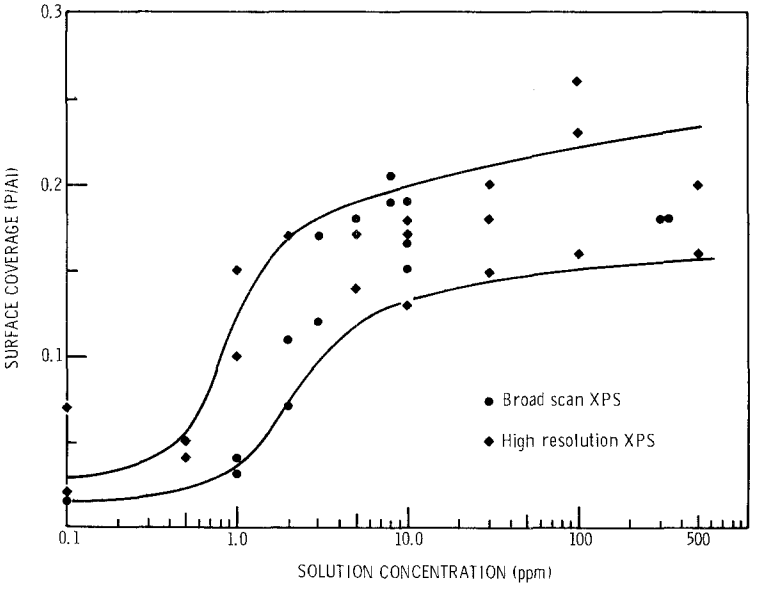

Figure 2 Surface coverage of NTMP-treated FPL oxide surface as a function of NTMP solution concentration.

TABLE I Inhibitor surface coverage at saturation as determined by XPS for 2024 aluminium adherends prepared by the FPL process

Inhibitor and treatment temperature	Surface coverage (P/Al ratio)
NTMP, RT	0.15-0.2
NTMP, 80° C	0.4
PA, RT	0.1

TABLE II G_{ISCC} obtained from wedge tests

Sample description	G_{ISCC} (in lb in^{-2})	($J\,m^{-2}$)
FPL	0.2-1.0	35-175
FPL + 2 ppm NTMP FPL + 10 ppm NTMP	0.6-2.5	105-440
FPL + 100 ppm NTMP	2-3	350-525
FPL + PA	0.25-0.7	45-120
Adhesive	6.5	1140

Wedge-test results (Fig. 4) obtained using FPL adherends treated with 10 ppm NTMP at 80° C show the same durability as adherends treated in the 10 ppm solution at room temperature. Results of wedge test experiments using PA-treated FPL adherends (Fig. 5), show that using this pretreatment procedure causes no improvement in bond durability.

Using the crack-length data generated by the wedge tests and Equation 4 we calculated the fracture energy, G. The crack velocity, v, was determined graphically from plots of crack length as a function of time; it is shown as a function of G in Figs. 6 to 9.

Fig. 8 includes data for the adhesive FM 123-2, which was obtained using PAA adherends sprayed with a corrosion-inhibiting primer prior to bonding. Use of PAA adherends* and a primer ensured that there were no contributions to crack extension from the adherend surface because the crack was completely cohesive through the adhesive.

The fracture energy analysis allows further evaluation of the inhibitor surface treatments. The G_{ISCC} value from Figs. 6 to 9 were tabulated (Table II). Unless G_{ISCC} is exceeded, crack propagation is below the level of experimental detectability. The significance of these results is discussed below.

3.3. SEM examination of failure surfaces

At the conclusion of the humidity exposure, the wedge test assemblies were separated. We observed that the original crack through the adhesive did not continue to propagate† in this manner after exposure to humidity. Instead, a new crack was initiated at the oxide/adhesive interface and continued at this location until crack arrest occurred.

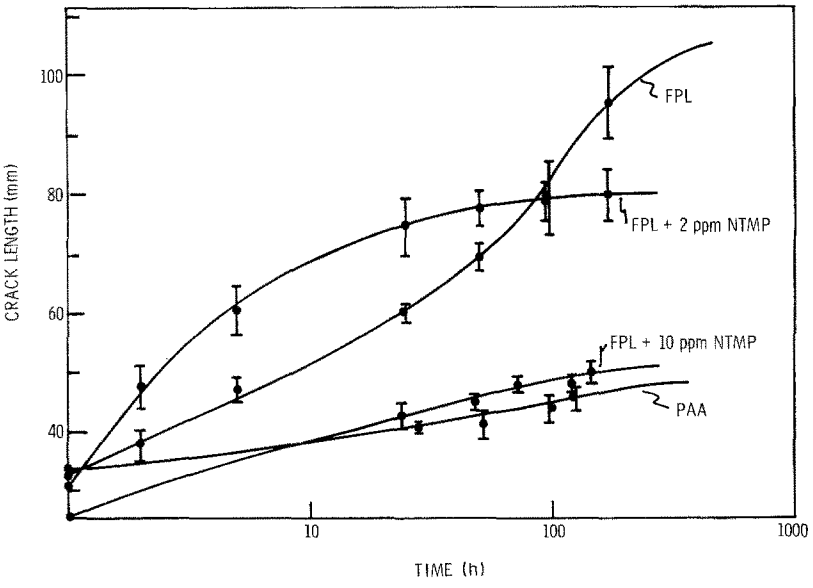

Figure 3 Crack length plotted against exposure time for FPL, NTMP-treated FPL, and PAA adherends.

*Use of a corrosion-inhibiting primer on FPL-prepared surfaces resulted in some interfacial crack propagation.
†In the absence of high humidity, the original crack did not propagate, even at 60° C.

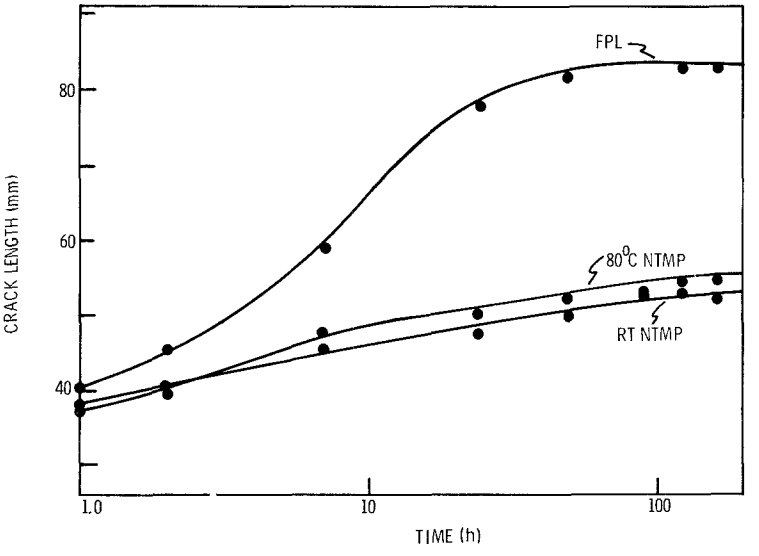

Figure 4 Crack length plotted against exposure time for FPL and NTMP-treated FPL adherends. NTMP solution concentration was 10 ppm.

Fig. 10 is a low magnification SEM micrograph of this initiation region. The raised adhesive indicates that the adhesive layer remained in one piece until separation of the adherends caused it to rupture.

A typical high magnification SEM micrograph taken from the aluminium side of a failure surface is shown in Fig. 11. The flake morphology is distinctive of boehmite.

3.4. XPS analysis of failure surfaces

To define the locus of failure more precisely, matching fracture surfaces were analysed using XPS; this analysis is presented in Table III. The matching FPL failure surface exhibited nearly identical surface composition, with substantial amounts of aluminium present on both sides of the fracture. In the case of the FPL adherend treated in NTMP at room temperature, the matching surface differed somewhat in composition, i.e. there was less aluminium and more carbon on the adhesive side of the failure than on the aluminium side.

There was a marked difference in the surface chemistry between the aluminium and adhesive sides on the FPL adherend treated in NTMP at 80° C. The aluminium failure surface was similar in composition to that of an untreated adherend

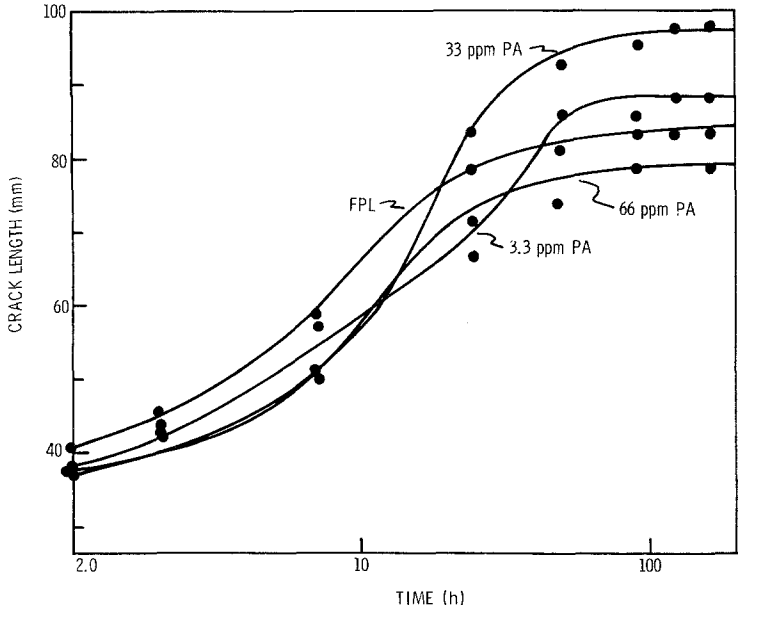

Figure 5 Crack length plotted against exposure time for FPL adherends and PA-treated FPL adherends.

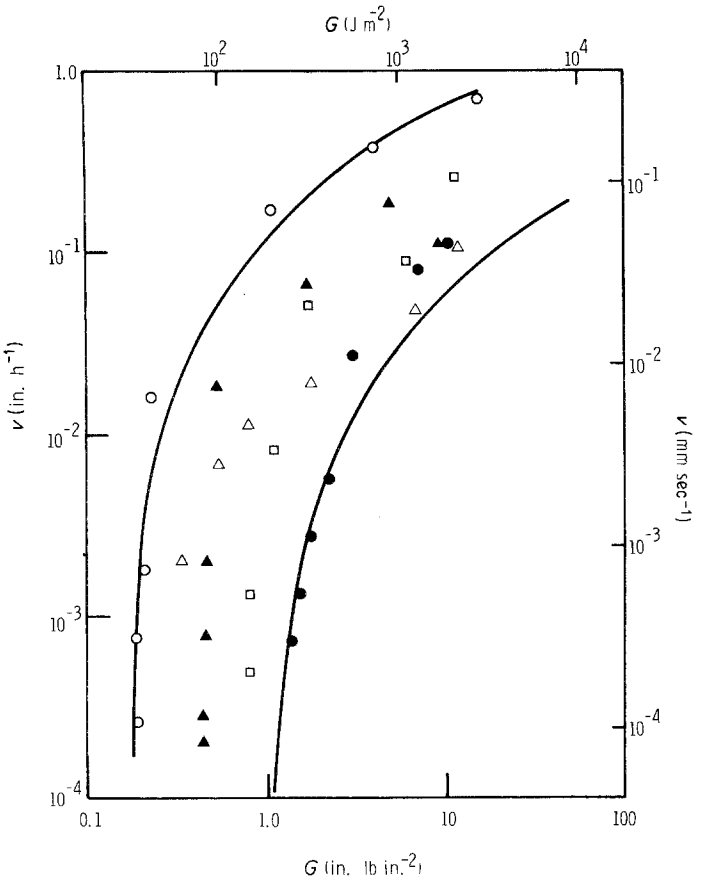

Figure 6 Crack velocity plotted against G for untreated FPL adherends.

(with the exception of the small amount of phosphorus), but the adhesive exhibited substantially less aluminium and more carbon than was seen on untreated surfaces. A small amount of phosphorus was present on both failure surfaces. The FPL adherends treated with 3.3 and 33 ppm PA were similar to the untreated FPL adherend and the samples treated with 66 ppm gave similar results to those of FPL adherends treated in NTMP at 80° C.

4. Discussion

The wedge test results for FPL adherends treated in room temperature NTMP solutions indicate that such treatments result in marked improvements in environmental durability, as measured by the final crack length after exposure to a humid environment. The observation of similar aluminium concentrations on both sides of the failure surface (Table III) of both the FPL and FPL + 10 ppm NTMP adherends confirmed previous observations

TABLE III Surface composition of failed surfaces as determined by XPS

Sample description	Element (at %)							
	Al		O		P		C	
	A*	B*	A	B	A	B	A	B
FPL	16	18	52	45	–	–	32	37
FPL + 10-ppm NTMP, RT	19	11	51	38	–	–	30	51
FPL + 10-ppm NTMP, 80° C	14	2.5	40	25	1	0.5	45	72
FPL + 3.3-ppm PA	18	15	46	43	–	–	36	42
FPL + 33-ppm PA	27	17	52	42	–	–	21	41
FPL + 66-ppm PA	25	2	49	25	0.6	–	25	73

*A is aluminium side of failure and B is matching adhesive side of failure.

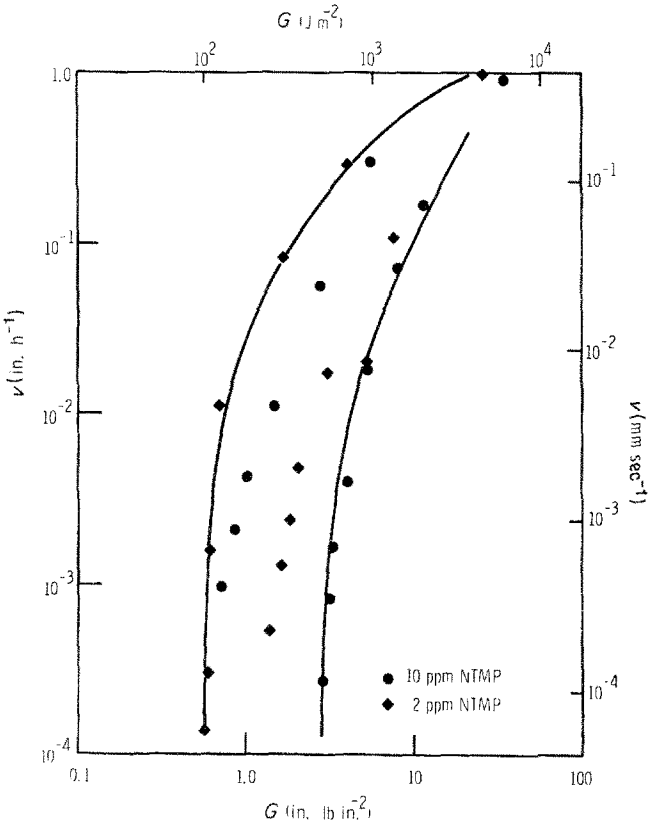

Figure 7 Crack velocity plotted against G for NTMP-treated FPL adherends.

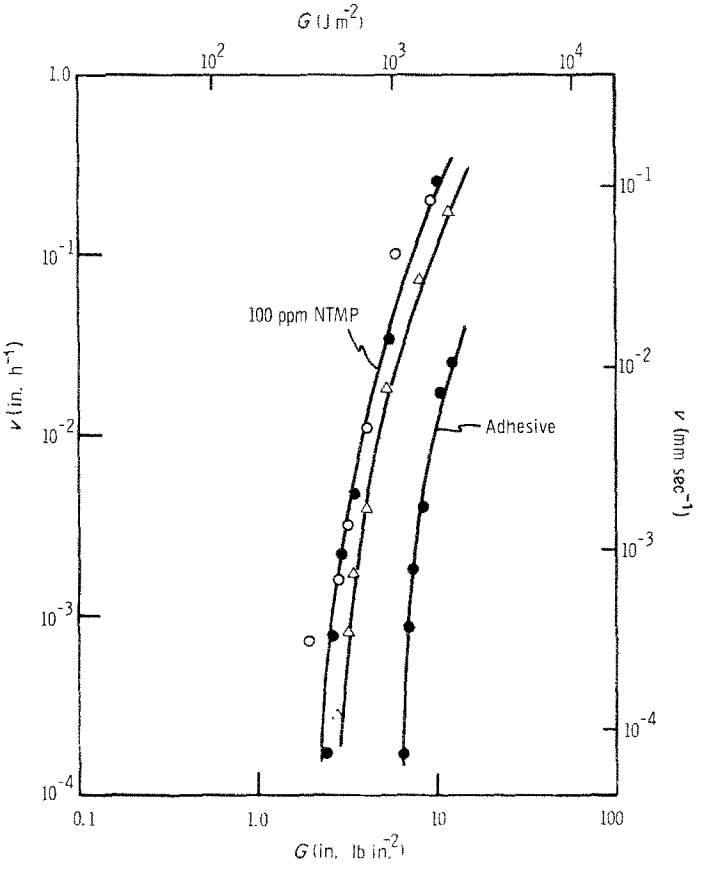

Figure 8 Crack velocity plotted against G for FPL adherends treated in 100 ppm NTMP solution and for the adhesive (FM 123-2).

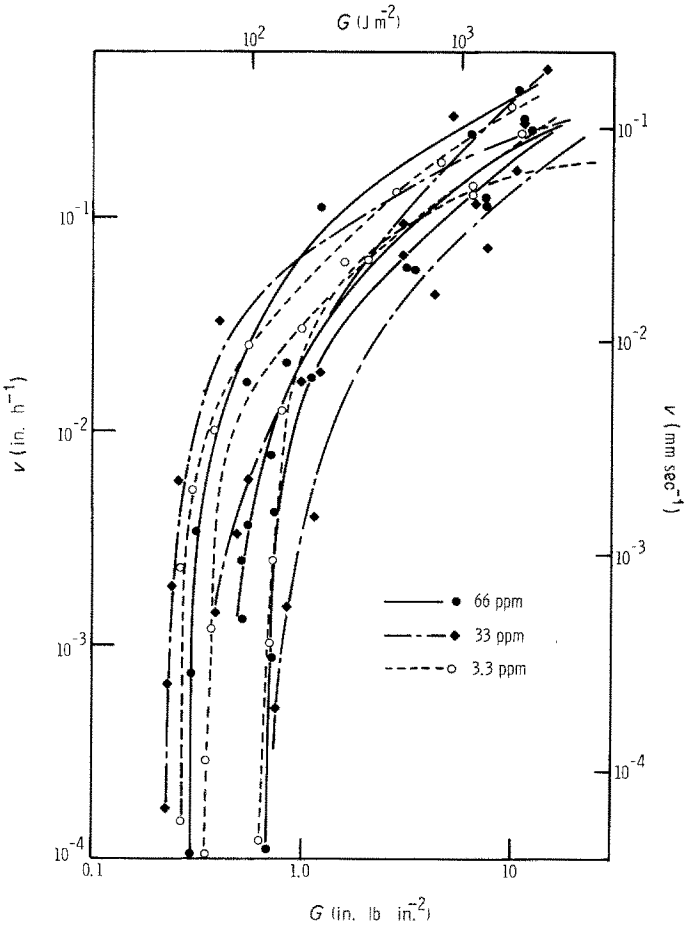

Figure 9 Crack velocity plotted against G for FPL adherends treated in PA.

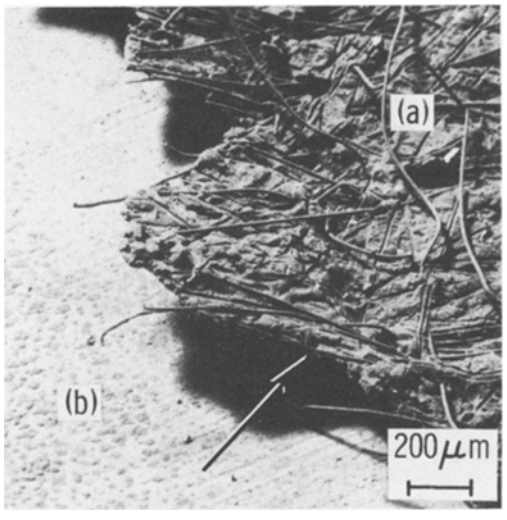

Figure 10 Macrograph of fracture surface at the position where stress concentration caused by crack in adhesive (a) initiates an interfacial failure (b). Arrow indicates initiation site of interfacial crack.

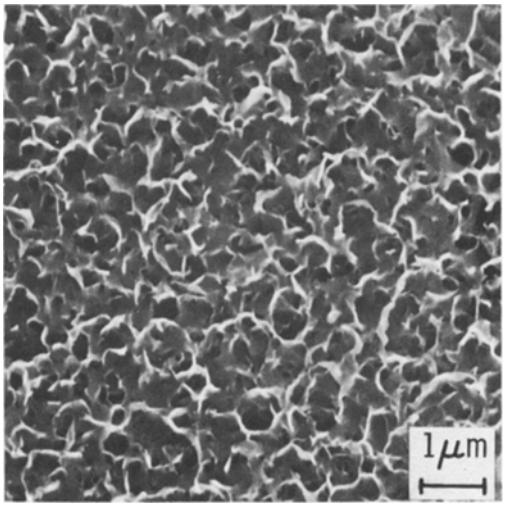

Figure 11 High resolution SEM micrograph of the side of the aluminium fracture surface.

[2] that the locus of failure was through a hydrated oxide layer. In the presence of moisture the original aluminium oxide is converted to aluminium hydroxide. The formation of boehmite from the initial oxide involves a lattice expansion, and the flake morphology characteristically adoped by the boehmite is considerably less dense than that of the original amorphous oxide. This oxide-to-hydroxide conversion disrupts the mechanical interlocking between the oxide and the adhesive, and the weak hydroxide layer provides a favourable path for crack propagation [2]. Previous work has shown that the adsorption of NTMP onto an FPL aluminium oxide surface increases the incubation time for oxide-to-hydroxide conversion [5]. Thus the improvements in bond durability that accompany NTMP surface pre-treatments most probably result from stabilization of the surface against hydration.

Maximum improvements in bond durability were associated with room-temperature saturation surface coverage (approximately monolayer). Higher coverage, such as that obtained by NTMP treatment at 80° C, did not further improve the bond durability, XPS results from the failure surface of 80° C-treated bondments showed that phosphorus was present on both the aluminium and adhesive sides, and the aluminium concentration on the adhesive side was quite low. This result suggests that failure occurred at least partially through the NTMP layer at the oxide/adhesive interface.

The wedge-test results for PA-treated adherends (Fig. 5) showed no decrease in crack extension compared with untreated adherends despite the effectiveness of PA treatments in inhibiting oxide-to-hydroxide conversion [6]. In the samples treated with 3.3 and 33 ppm PA, the inhibiting effect of PA was apparently not adequate to prevent the oxide-to-hydroxide reaction; large amounts of aluminium are found on both the aluminium and the adhesive sides of the failure surfaces (Table III), indicating that the locus of failure was through the hydration-weakened oxide layer. The XPS results from the fracture surfaces in the case of the 66-ppm PA treatment suggest that the crack propagated at the PA film/adhesive interface, because little aluminium was found on the adhesive side of the failure and a small amount of phosphorus was detected on the aluminium side. Although PA inhibits the hydration reaction, the PA/adhesive bonds are not resistant to attack by moisture and, therefore, provide an easy path for crack propagation.

It is interesting to compare the results obtained with 66 ppm PA-treated adherends with those for adherends treated in 10 ppm NTMP at 80° C. Both treatments appear to be highly effective in retarding oxide-to-hydroxide conversion. In both cases, only very small (~ 2 at%) amounts of aluminium were found on the adhesive side of the failure, indicating that failure had not occurred through a hydrated oxide layer. Rather, failure was associated with the inhibitor films themselves. However, despite an apparently common locus of failure, the two treatments produced markedly different wedge-test results. In the case of the 80° C NTMP treatment, substantial improvements in bond durability were seen, which suggests that the NTMP/adhesive chemical bond is quite resistant to moisture attack. No improvement resulted from treatments in 66-ppm PA indicating that the PA/adhesive chemical bond is not moisture resistant.

These results suggest that, to obtain improvements in bond durability, it is important not only to inhibit hydration, but also to produce good chemical bonding between the adherend and the adhesive. Although a definitive model has not yet been proposed for the adsorption mechanism of NTMP molecules to an oxide surface, the NTMP molecule has many functional groups available for bonding (six (OH) groups and the lone electron pair on the nitrogen atom) and not all will be required for adsorption to the oxide. The phosphoric acid molecule, on the other hand, has fewer functional groups available for bonding (three (OH) groups) and is also a very small and thus not very flexible molecule. Even if adsorption to the oxide does not utilize the full bonding potential of the moelcule, any remaining sites may not be favourably oriented for bonding to the adhesive. Thus, although it is easy to envision NTMP acting as a coupling agent between the adherend oxide and the adhesive, it is difficult to imagine PA in the same role.

If chemical bonding between the adherend and the adhesive is important, then what accounts for the excellent durability of PAA adherends? The P/Al ratio of PAA adherends and PA-treated FPL adherends are similar and in both cases the phosphorus is derived from phosphoric acid. However, the oxide morphologies produced by the FPL and PAA processes are significantly different [1]. Oxides produced by the PAA process interlock

with the adhesive through a substantially thicker oxide layer than that produced by the FPL process. Physical interlocking should thus be more efficient in the PAA case and bond performance consequently less dependent on chemical coupling between the oxide and the adhesive than would be the case for FPL adherends. Any degradation between a PA-like film and the adhesive should have little effect on the bond durability of PAA adherends because the substantial interlocking of oxide and adhesive will retard crack propagation. At the same time, the phosphorus groups on the PAA oxide stabilize it against hydration, resulting in excellent bond durability.

The fracture energy analysis of the wedge-test data allows improvements in bond durability conferred by the inhibitor treatment to be assessed quantitatively. The values of G_{ISCC} in Table II are, of course, specific to the test conditions used and the assumptions made in their calculation. However, they do indicate that NTMP treatment results in a four-fold average increase in G_{ISCC}.

The value of 1.1 kJ m^{-2} for the G_{ISCC} of the adhesive in Table II is obtained from wedge tests in which the failure was cohesive, i.e. there was no contribution from the adherend oxide. Thus, this value reflects only the behaviour of the adhesive under stress in a warm humid environment.

In all other cases, insertion of the wedge test assemblies into the warm humid environment resulted in the initiation of a crack at or near the oxide/adhesive interface. This initiation of an interfacial crack in pre-cracked statically loaded specimens in response to humid environment exposure has been described by other investigators [8]. The initiation of the interface crack (in common with its propagation) is apparently due to hydration of the oxide and the associated breakdown of interface integrity. If moisture is excluded from the interface, or the interface stabilized, then interfacial failure does not occur.

In summary, hydration inhibitors can be used to improve the bond durability of adherends etched in FPL. Use of NTMP improves the durability of FPL-prepared 2024 aluminium adherends to the point where they behave in nearly the same manner as adherends prepared with the PAA process. Analysis of the results suggest that an inhibitor's effectiveness depends on both its ability to inhibit the conversion of aluminium oxide to hydroxide and to form chemical bonds with the adhesive.

Acknowledgements

We gratefully acknowledge the technical assistance of A. I. Desai and R. C. Butler and valuable discussions with G. D. Davis and D. K. McNamara. We also thank the Office of Naval Research and the Army Research Office, Durham for jointly sponsoring this study under contract N00014-80-C-0718.

References

1. J. D. VENABLES, D. K. McNAMARA, J. M. CHEN, T. S. SUN and R. L. HOPPING, *Appl. Surf. Sci.* **3** (1979) 88.
2. J. D. VENABLES, D. K. McNAMARA, J. M. CHEN, B. M. DITCHEK, T. I. MORGENTHALER, T. S. SUN and R. L. HOPPING, Proceedings of the 12th National SAMPE Symposium, Seattle, Washington, October 1980 (SAMPE, Azusa, California, 1980) p. 909.
3. D. A. VERMILYEA and W. VEDDER, *Trans. Faraday Soc.* **66** (1970) 2644.
4. G. D. DAVIS, T. S. SUN, J. S. AHEARN and J. D. VENABLES, *J. Mater. Sci.* 17 (1982) 1809.
5. J. S. AHEARN, G. D. DAVIS, T. S. SUN and J. D. VENABLES, in "Adhesion Aspects of Polymeric Coatings", edited by K. L. Mittal (Plenum Publishing Corporation, 1983) p. 281.
6. J. S. AHEARN, G. D. DAVIS, A. I. DESAI and J. D. VENABLES, Martin Marietta Laboratories, Baltimore, MD, Technical Report MML TR 81-46c. October (1981).
7. D. BROEK, "Elementary Engineering Fracture Mechanics" (Sijthoff and Noordhoff, The Netherlands, 1978) p. 154.
8. M. H. STONE and T. PEET, Royal Aircraft Establishment Tech. Memo MAT 349, July (1980).
9. R. L. PATRICK, J. A. BROWN, L. E. VERHOEVEN, E. J. RIPLING and S. MOSTOVOY, *J. Adhesion* **1** (1969) 136.

Received 8 April
and accepted 13 May 1983